

International Journal of River Basin Management

Publication details, including instructions for authors and subscription information:
<http://www.tandfonline.com/loi/trbm20>

Flood generation and classification of a semi-arid intermittent flow watershed: Evrotas river

Ourania Tzoraki ^a, David Cooper ^b, Thomas Kjeldsen ^c, Nikolaos P. Nikolaidis ^d, Christos Gamvroudis ^e, Jochen Froebrich ^f, Erik Querner ^g, Francesc Gallart ^h & Nikolaos Karalemas ⁱ

^a Technical University of Crete (TUC), Chania, Greece

^b Centre for Ecology and Hydrology (CEH), Bangor, United Kingdom

^c Centre for Ecology and Hydrology (CEH), Wallingford, United Kingdom

^d Technical University of Crete (TUC), Chania, Greece

^e Technical University of Crete (TUC), Chania, Greece

^f Centre for Water and Climate (CWK), Alterra, Wageningen, The Netherlands

^g Centre for Water and Climate (CWK), Alterra, Wageningen, The Netherlands

^h Institute of Environmental Assessment and Water Research (IDAEA), CSIC, Barcelona, Spain

ⁱ Faculty of Geology, University of Athens, Greece

To cite this article: Ourania Tzoraki , David Cooper , Thomas Kjeldsen , Nikolaos P. Nikolaidis , Christos Gamvroudis , Jochen Froebrich , Erik Querner , Francesc Gallart & Nikolaos Karalemas (2013): Flood generation and classification of a semi-arid intermittent flow watershed: Evrotas river, *International Journal of River Basin Management*, 11:1, 77-92

To link to this article: <http://dx.doi.org/10.1080/15715124.2013.768623>

PLEASE SCROLL DOWN FOR ARTICLE

Full terms and conditions of use: <http://www.tandfonline.com/page/terms-and-conditions>

This article may be used for research, teaching, and private study purposes. Any substantial or systematic reproduction, redistribution, reselling, loan, sub-licensing, systematic supply, or distribution in any form to anyone is expressly forbidden.

The publisher does not give any warranty express or implied or make any representation that the contents will be complete or accurate or up to date. The accuracy of any instructions, formulae, and drug doses should be independently verified with primary sources. The publisher shall not be liable for any loss, actions, claims, proceedings, demand, or costs or damages whatsoever or howsoever caused arising directly or indirectly in connection with or arising out of the use of this material.



Research paper

Flood generation and classification of a semi-arid intermittent flow watershed: Evrotas river

OURANIA TZORAKI, *Technical University of Crete (TUC), Chania, Greece.*

Email: rania.tzoraki@enveng.tuc.gr

DAVID COOPER, *Centre for Ecology and Hydrology (CEH), Bangor, United Kingdom.*

THOMAS KJELDSSEN, *Centre for Ecology and Hydrology (CEH), Wallingford, United Kingdom.*

NIKOLAOS P. NIKOLAIDIS, *Technical University of Crete (TUC), Chania, Greece.*

CHRISTOS GAMVROUDIS, *Technical University of Crete (TUC), Chania, Greece.*

JOCHEN FROEBRICH, *Centre for Water and Climate (CWK), Alterra, Wageningen, The Netherlands.*

ERIK QUERNER, *Centre for Water and Climate (CWK), Alterra, Wageningen, The Netherlands.*

FRANCESC GALLART, *Institute of Environmental Assessment and Water Research (IDAEA), CSIC, Barcelona, Spain.*

NIKOLAOS KARALEMAS, *Faculty of Geology, University of Athens, Greece.*

ABSTRACT

Hourly water level measurements were used to investigate the flood characteristics of a semi-arid river in Greece, the Evrotas. Flood events are analysed with respect to flood magnitude and occurrence and the performance of Curve Number approach over a period of 2007–2011. A distributed model, Soil and Water Assessment Tool, is used to simulate the historic floods (1970–2010) from the available rainfall data, and the performance of the model assessed. A new flood classification method was suggested the Peaks-Duration Over Threshold method that defines three flood types: 'usual', 'ecological' and 'hazardous'. We classify the basin according to the flood type for the most serious past simulated flood events. The proportion of hazardous floods in the main stream is estimated to be 5–7% with a lower figure in tributaries. Flood Status Frequency Graphs and radar plots are used to show the seasonality of simulated floods. In the Evrotas, the seasonality pattern of hazardous flood is in agreement with other studies in Greece and differs from other major European floods. The classification in terms of flood types in combination with flood type seasonality is identified as an important tool in flood management and restoration.

Keywords: Temporary streams; floods; river basin; SWAT model; flood seasonality; flood type; Greece

1 Introduction

Many catastrophic flood events causing serious damage and threatening human life are recorded each year in the Mediterranean area. In the future under projected climate change, an increase in flood frequency and magnitude is expected (Van

Lanen *et al.* 2007). In an area where water limitation is a major concern, a priority for river basin managers is to estimate and improve the retention of rainwater in the catchment while also controlling the effect of floods. This requires improved understanding of the flood generating processes for the successful design of the flood relief and related schemes. Catchment

Received 2 October 2012. Accepted 17 January 2013.

ISSN 1571-5124 print/ISSN 1814-2060 online
<http://dx.doi.org/10.1080/15715124.2013.768623>
<http://www.tandfonline.com>

characteristics including topography (elevation, area, slope, and drainage density), spatial variation of soil types, geological substrate, and vegetation density all play a role in determining catchment hydrology in semi-arid catchments (Belmonte and Beltrán 2001, Marchi *et al.* 2010), and the magnitude and occurrence of floods.

In Mediterranean rivers, the hydrological regime is characterized by flash floods (Vivoni *et al.* 2006), fluctuations in floodplain inundation (Tockner *et al.* 2000), spring baseflow (Rimmer and Salinger 2006) and periods where there is no flow (Nikolopoulos and Anagnostou 2011). The behaviour of such rivers is difficult to study and predict (Gallart *et al.* 2008, Kirkby *et al.* 2011) due to limited flow data, difficulties in instrument installation and operation in such environments (Tzoraki *et al.* 2007, Kourgialas *et al.* 2010, Moraetis *et al.* 2010), and insufficient precipitation measurement in an area where rainfall is highly variable in time and space. Post-event analysis of 25 example floods (Marchi *et al.* 2010), strengthened the belief that available methodologies for flood prediction are highly uncertain and new approaches should be developed for flood analysis. Flood events in perennial rivers have been studied by Gaume *et al.* (2009) with a view to creating an atlas of extreme flash floods across Europe. They observed a strong seasonality to flood occurrence, revealing different forcing mechanisms in each region.

The estimation of flood distribution characteristics is ideally based on a long-term flow record. However, such a record is often not available; in which case flood estimates can be derived using a model based on precipitation records as drivers and catchment characteristics as response moderators. The use of such a model introduces additional uncertainty into flood characterization because of uncertainty in the drivers and moderators themselves, and in the relationship between them and the flood response.

There are a variety of methods of relating flood occurrence and magnitude to precipitation measurements through modelling. One widely used method of estimating the runoff potential volume, highly correlated with flooding, for individual rainfall events in basins with perennial flow is the Curve Number (CN) approach (Hawkins *et al.* 2009). This approach essentially condenses catchment moderating (ignoring any drainage flow from groundwater) characteristics into a single parameter in a nonlinear relationship between event precipitation and event flood characteristics. CNs may be tabulated against other directly measurable catchment characteristics, although they may also be estimated using available precipitation and flood data by a calibration procedure. The CN approach (with a variety of modifications) is used in numerous applications and mathematical models such as Soil and Water Assessment Tool (SWAT) (Arnold *et al.* 1988), Hydrological Simulation Program – Fortran (HSPF) (Bicknell *et al.* 2001) and Enhanced Trickle Down Model (ETD) (Nikolaidis *et al.* 1994). The method was developed for US river basins (Hawkins *et al.* 2009), and still requires verification in other parts of the world. For instance,

the CN method captures poorly the temporal runoff dynamic of monsoonal climates and areas dominated by complex hydrogeology (White *et al.* 2011). Also in karstic basins, floods are initiated only if a rainfall threshold is exceeded (Kourgialas *et al.* 2010), supporting the assumption that the local geology is a key factor in flood generation process. The authors identified three flash flood classes depending on antecedent soil moisture conditions (Kourgialas *et al.* 2010). A modified CN equation in the SWAT model gave satisfactory streamflow predictions of Ethiopian and Catskill Mountains river basins (White *et al.* 2011). Physical properties of the soil are affected by rainfall events enhancing runoff velocity, transport capacity and reducing the lag time of a flash flood event (Fohrer *et al.* 1999, Kourgialas *et al.* 2011).

We analyse flood events with respect to flood magnitude and occurrence and the performance of CN approach to flood simulation in the Evrotas catchment, Greece using high frequency available flow data of the period 2007–2011. The SWAT distributed rainfall–runoff model is calibrated and validated on data over the period 2000–2011. The model is then used with precipitation data from 1970 to 2000 to generate a historic flow record over this period. We delineate homogenous regions according to flood classes for the most serious past simulated flood events, identifying the areas of high flood risk. Finally, we assign flood classes frequency and location of occurrence.

1.1 Catchment characteristics

Our study catchment, the Evrotas, like many rivers in the Mediterranean region, is a temporary river with intermittent flow in the main stream and many tributaries. The basin (Figure 1) is located in the south-eastern Peloponnese (Greece) covering an area of 2,050 km², with a main stream length of 90 km. The basin has a Mediterranean climate with mild or cold winters and prolonged hot and dry summers with a mean annual temperature of 18.4°C at Sparta. Monthly mean temperatures are typically 10.2°C in winter and 27.5°C in summer at this location.

The catchment is bounded by the Taygetos (2407 m above MSL) and Paronos (1940 m above MSL) mountains from which numerous ephemeral and intermittent streams discharge into the river network. The main tributaries are the Oinountas, Magoulitsa, Gerakaris, Kakaris, and Rasina (intermittent flow), Mariorema, Xerias (episodic flow). Some 40% of the catchment area is above 600 m elevation, 45% between 150 and 600 m, and 13% between sea level and 150 m. The land surface is approximately 59% forest, 40% agricultural and 1% urban. The population is 66,000, the largest town being Sparta with 18,000 inhabitants. The main activities in the catchment are agriculture (livestock-rearing and a variety of crops including olives and citrus fruits) and small-scale food-processing industries.

The Taygetos and Paronos mountains are largely karstic, but with areas of impermeable formations. A series of low-transmissivity alluvial fans, restricted to the piedmont zone adjacent to

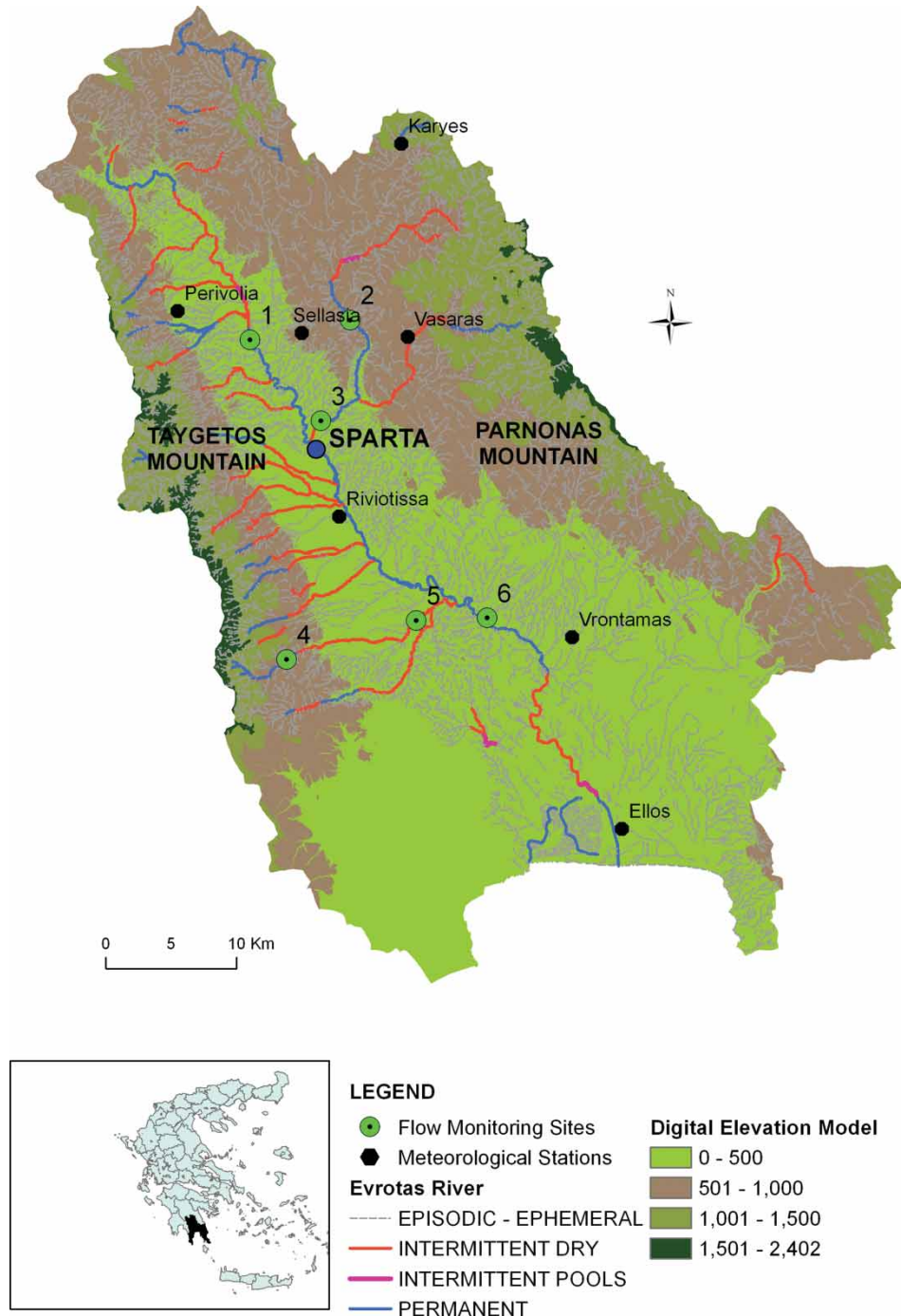


Figure 1 High risk flood disaster regions of Lakonia (data from the Civil Protection Office of Lakonia Prefecture) (black polygons: meteorological stations; green circles: study sites – 1. Vivari, 2. Oinountas Vasaras, 3. Oinountas Kladas, 4. Rasina Koumousta, 5. Rasina Airport, 6. Vrontamas).

the east edge of the Taygetos mountains, comprise significant water storage. The Taygetos karst has high transmissivity (10^{-3} – 10^{-4} $m^2 s^{-1}$) and recharges the alluvial fans and associated aquifer north-west of Sparta. The unsaturated zone in this region has thickness 20–30 m with saturated hydraulic conductivity varying between 7×10^{-7} – 8×10^{-5} ms^{-1} (Antonakos and Lambrakis 2000). The Sparta aquifer is penetrated by numerous wells used to provide water for irrigation.

Long sections of the river have intermittent flow, influenced by the local geology, low rainfall, abstraction and high

evaporation. The percentages of the total river network having permanent and intermittent flow, respectively, are 3.5% and 4.3% (total river network 5143 km). The highest part of the stream network (92% of river total length) has rain-generated flow which is episodic and appears only during a rain event. The main causes of river bed desiccation are the steep topography of the terrain, the karst geology and groundwater abstraction for irrigation. The steep slopes of the Taygetos mountain, the scarce vegetation of the high elevation grassland areas in combination with the human alteration of the

Table 1 Main physiographic and flow characteristics of the sub-basins.

	Area (km ²)	Mean elevation (m)	Relief (m)	Ratio karst area/total area (km ²)	Discharge (m ³ s ⁻¹)	Available monthly flow data
Vivari	394.1	305	1270	0.41	1.84 (\pm 2.0)	1986–2011
Oinountas Vasaras	164.4	685	516	0.41	0.32 (\pm 0.30)	1995–2011
Oinountas Kladas	349.8	211	1337	0.35	0.31 (\pm 0.31)	2008–2011
Rasina Koumousta	28.5	954	2208	0.66	0.58 (\pm 0.47)	2009–2011
Rasina airport	55.8	166	2244	0.37	0.45 (\pm 0.45)	2009–2011
Vrontamas	1348	181	2267	0.45	3.62 (\pm 4.23)	1973–2011

natural drainage paths result in floods with significant bank erosion and sediment transport.

1.2 Catchment hydrological measurement

There are six flow-gauging stations on the Evrotas and its tributaries, as shown in Figure 1. Two of these, at Vrontamas and Vivari, are on the main river; two are on the Oinountas and two on the Rasina tributaries. As indicated in Figure 1, the six sub-basins are partially nested. Automatic level-loggers, Onset Computers and HOBO pressure transducers (U20-001-04) were installed in 2004 to continuously monitor water level at 15-min intervals at these sites, with discharge measured monthly in order to estimate rating curve equations. In addition, monthly measurements of flow at Vivari and Vrontamas are available for 1974–2011.

In the main Evrotas river, the reach between Vivari (Site 1, Figure 1) and Vrontamas (Site 6) defines a length of permanent stream and collects the drainage of the numerous ephemeral and temporary flow tributaries. Just above the Vivari gauging site, multiple springs (mean annual outflow $1.05 \pm 0.9 \text{ m}^3 \text{ s}^{-1}$, 1974–2010) provide the permanent flow at this site. The Vrontamas gauging station measures the drainage of the whole catchment and downstream of that point the river water is gradually lost to bed infiltration as the river enters a karstic gorge. The Oinountas sub-catchment drains the NW Paronias mountain and is the longest Evrotas tributary. Much of the river basin geology is schist with low permeability and flooding vulnerability. Two water-level sampling sites were selected in the Oinountas sub-catchment. Vasaras (Site 2), located in the north-east part of the sub-catchment with a drainage area of 164.4 km² and an impermeable substrate. The second gauge is located at Kladas just before the confluence with the main stream (Site 3), thus measuring the flow of the entire sub-catchment with its varying hydrogeology. The Rasina drains a part of the Taygetos mountain, and has two level-loggers installed; the first upstream at a location that drains the infiltration excess of the karst (Site 4), and the second close to the confluence with the Evrotas main stream (Site 5). For the period of 2000–2010, the maximum daily gross stream power was estimated as 42.5 Kwh for the Vivari, and for the Oinountas, Rasina and Vrontamas 9.2, 9.9 and 48.5 Kwh, respectively. The high-gross stream power value of Vivari indicates the high-flood risk potential of Taygetos streams that may be due to steep topography. Indeed, in

the short-time period of 7 years (1999–2006), 33 different areas have been subject to floods by five hazardous flood events (Nikolaidis 2009).

Daily precipitation has been measured since the 1970s at six stations: Ellos (4 m elevation), Riviotissa (163.5 m), Vrontamas (280 m, operating since 1953), Perivolia (490 m), Sellasia (590 m) and Vasaras (646 m) (Figure 1). The mean annual precipitation measured at these sites ranges from 1300 mm (Perivolia) to 540 mm (Elos) and the average annual precipitation over the whole catchment is 800 mm (estimated by the Thiessen method for the hydrologic years 2000–2007). The annual precipitation in Vasaras is 770 mm, in Riviotissa 930 mm and Vrontamas station 410 mm (average annual 1954–2010). A precipitation duration curve for Vrontamas constructed from daily data (excluding days of no rain) for the period 1990–2011 shows the 50th, 90th and 99th percentiles have been estimated as 4–9, 19–37 and 47–88 mm, respectively. Most precipitation falls between October and February (often as snow over the mountains) with, for example, 78% of the precipitation at Vrontamas falling in that period. Based on data from these six stations, the catchment shows a decline in recorded precipitation from west to east and from north to south.

The Evrotas basin has no automatic weather station (AWS) measuring hourly precipitation records, limiting our information on the duration and intensity of rainfall. There is an AWS located at Karyes (elevation 950 m, Figure 1), where, although the available data are daily, there are records of rain duration (in hours). For 367 rain events for the period of 2006–2010, the mean precipitation depth was 8.7 mm/event, with a mean event duration of 9 h (\pm 7.7 h) and a mean intensity is 1.8 mm h⁻¹.

For modelling purposes, the main physiographic characteristics were estimated for each gauged sub-basin, including drainage area, mean elevation, basin relief and fraction of the karst area (Table 1) using digital thematic maps.

1.3 Hydrological response

The runoff coefficient (RC) (the ratio of flood volume to precipitation volume) was estimated in each sub-catchment as the mean value across all measured flood events of the study period. The estimated RCs were 0.22 for the Vivari, 0.17 for Rasina Koumousta, 0.28 for Rasina airport and 0.26 for Vrontamas. At

Oinountas Vasaras, the karstic geology enhances infiltration and reduces runoff generation to around 4% ($\pm 6\%$). In the Rasina, the mean annual flow decreases downstream possibly due to water abstraction, even though in flood events, the RC increases downstream and significant baseflow contributes to the stream. In smaller events, only a minor fraction of the precipitation volume generates runoff (26% for the whole basin, measured at Vrontamas) and precipitation mainly contributes to infiltration, evapotranspiration and transmission losses. Runoff analysis indicates that the sub-basins most vulnerable to flooding are the Vivari, Rasina and Vrontamas. The low-RCs of the Evrotas basin accords with other studies from the Mediterranean region, for example. In Spain, in the Valencia region, where a significant deficit between precipitation and discharge was observed (0.7–17% RC) and in Libya for a calcareous basin the RC was estimated 0.22–20.2% (Belmonte and Beltrán 2001). It was reported relatively low values of event RC (0.07–0.21) in the analysis of flush flood events on the semi-arid Walnut Gulch basin. Similar RCs 0.02–0.38 were reported for the arid catchment in Oman (McIntyre *et al.* 2007). Higher RC (0.41 ± 0.22) values appear more typical of extreme flash floods in perennial rivers in Europe by Marchi *et al.* (2010).

In order to understand the flood response of intermittent streams, hydrographs of selected events at upstream and downstream locations of the studied sub-catchments are presented in Figures 2 and 3. The estimated hourly flows were normalized to

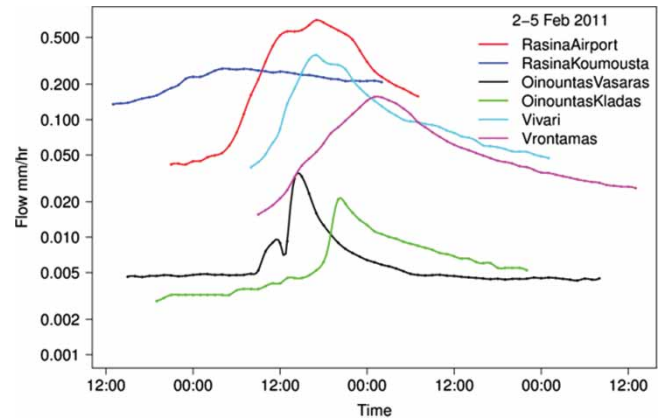


Figure 3 Hydrographs for all sites for the event of 2–5 February 2011 (log scale).

runoff sheet depth (mm) to compensate for the diverse drainage areas, and the Time-to-Peak, defined as the time of the initial rise to attainment of peak discharge, was estimated. The smooth shape of the Rasina Koumousta hydrograph for four storm events shows that the surface runoff has a subdued response to rain events (Figure 2). Previous studies in Taygetos mountain karstic terrain indicated that the infiltration process into the karst is responsible for almost 50% of rain water losses (Tzoraki *et al.* 2011) thus enhancing the retardation of the rain water and preventing flash floods. The hydrograph at Rasina Airport, downstream of

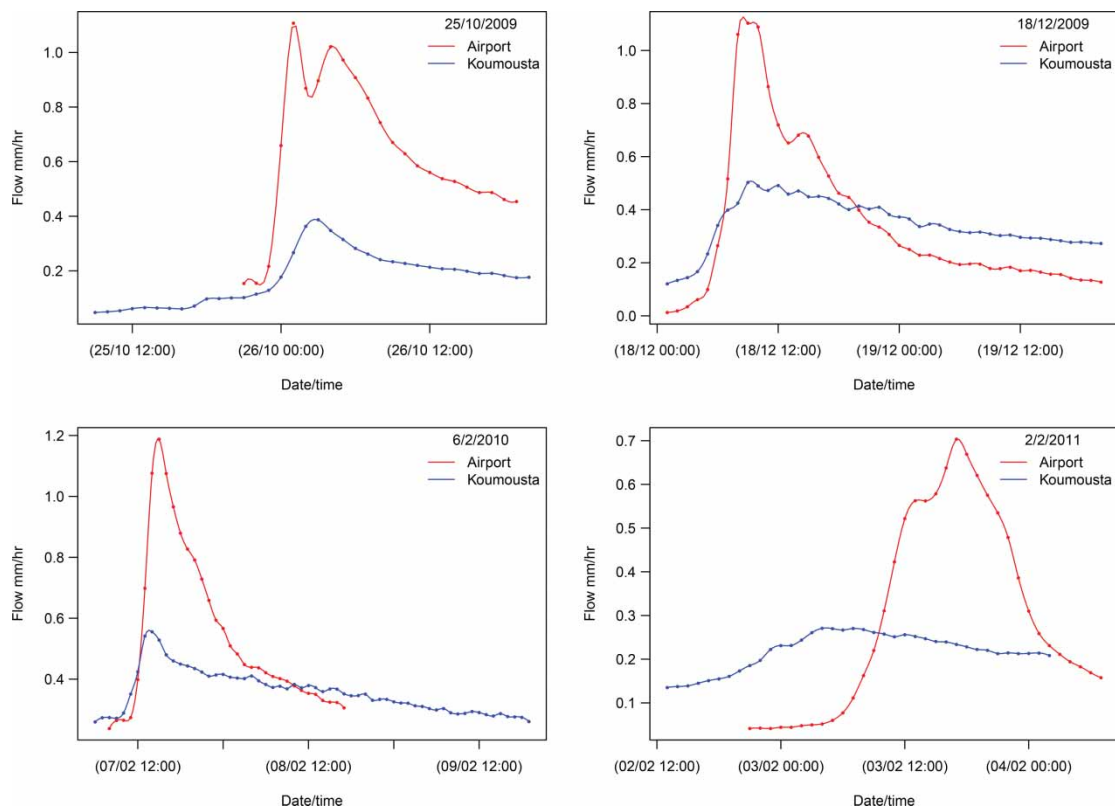


Figure 2 Hydrographs of four selected rain events for the Rasina stream, showing the hydrograph evolution from upstream areas (Koumousta) to downstream (Airport).

Koumousta, shows a more pronounced response, interpreted as due to a dense drainage network enhanced by contributions from numerous karstic springs, superimposed on additional flow from the low-permeability alluvial and phyllitic substrate.

The Oinountas, Vasaras and Kladas are also intermittent flow streams (Figure 3). Vasaras hydrographs are flashy with steeper limbs of the hydrographs and higher flow peaks. For instance, for the rain event of 3 February 2011, the Time-to-Peak was 27 h (corresponding to a rain of 40.1 mm) in Vasaras and downstream at Kladas 32 h (66.5 mm rain) and the flood volume is reduced (Figure 3). The hydrograph pattern of the Oinountas basin can be attributed to groundwater flow through the karst with its numerous faults as well as abstractions. In contrast to the Rasina, the upstream hydrographs on the Oinountas show greater discharge than downstream for flood events. The Vivari hydrographs (Figure 3) show steep rising limbs that reflect a prompt runoff generation mechanism and mild recession limbs that include the karst precipitation excess and the alluvial subsurface flow and the infiltration excess. Finally, the Vrontamas hydrograph shows the response of the variable hydrologic type streams and the complex geological structure of the catchment.

The mean recorded rain event duration at Karyes (9 ± 7.7 h) indicates that in most cases, the Evrotas precipitation events have a duration less than one day. The lack of sub-daily precipitation data causes major uncertainty in the estimation of the effective rainfall and the response time of the basin (the time between the centre of gravity of the hyetograph and the peak of the hydrograph). We can only estimate the time to peak of the hydrograph from the available hourly flow data.

During the gauging station operation period (2007–2011), only a small number of floods were recorded due to the extreme seasonal nature of rainfall in the region and the extreme drought year of 2007. For example at Vivari, a total of 14 flood events were observed during four hydrologic years (Table 2) with flood volume between 0.09–7.5 hm³. The duration of the flood varied between 17 and 84 h and the maximum hourly peak hydrograph was estimated to be 38.8 m³ s⁻¹ (or 21 times the mean annual flow). The floods throughout the basin that were recorded were not extreme with the exception of one flood event at the Vrontamas gauging station over the period of 25 February–14 March 2010 with a flood peak of

209.2 m³ s⁻¹ (58 times the mean annual flow). In the Oinountas, only 8 events were recorded at Vasaras, although downstream at Kladas 19 events were captured for the same time period reflecting the spatial variation of rainfall and the high infiltration capacity of the upstream karstic part of the catchment. Vrontamas recorded the largest number of events (21 events, Table 2) and also more complex multiple events as a result of spatial and temporal variation in rainfall contributing to the numerous streams (temporary, episodic and permanent) feeding the main channel. It is notable that at Vrontamas during the operational period only 21 flood events were recorded when (from the meteorological station) 414 of 1278 days in Vrontamas recorded rainfall. This demonstrates the high variability in the rainfall pattern and the frequent lack of an observed direct response of surface runoff to rain events.

Table 2 shows the period of 15-min flow monitoring, storm events and their associated statistics.

In characterizing the flood response, we first investigate if the between-event variation in observed peak flow (Q_p) in each sub-catchment can be described using the relationship between peak-flow and flood volume, T_v , and flood duration, D . The equation proposed by Sharma and Murthy (1998) is

$$Q_p = c \left(\frac{T_v}{D} \right)^a, \quad (1)$$

where the parameters c and a are indexes of hydrograph shape.

Eq. 1 gives $R^2 > 0.8$ with the exponent a (range 0.954–1.1586) declining nonlinearly in relation to drainage area. Table 3 shows the variability in parameter estimates between sites.

To further characterize the flood response, we have sought to relate runoff volume to precipitation using the widely used ‘CN’ approach. This approach is based on the empirical equation

$$F = \frac{(P - I_a)^2}{(P - I_a) + S}, \quad (2)$$

where for each rainfall and flood response event, S is the basin storage in mm, P the precipitation and I_a the initial abstraction in mm, assumed to be equal to $0.2 \times S$, and F

Table 2 Rainfall–runoff events for the six gauging stations.

Station	Time interval	Events number	Precipitation (mm)	Flood duration (D , h)	Flood volume (T_v , hm ³)	Peak of hydrograph (Q_p , m ³ s ⁻¹)
Vivari	11/2007–3/2011	14	9.2–70.8	14–64	0.09–7.5	2.8–38.8
Oinountas Vasaras	9/2009–4/2011	8	10.9–54.0	7–27	0.02–0.7	1.1–127.5
Oinountas Kladas	6/2009–4/2011	19	2.5–106.7	10–401	0.006–4.2	0.3–17.8
Rasina Koumousta	10/2009–4/2011	19	22.9–145.2	19–104	0.04–0.9	0.4–48.8
Rasina airport	10/2009–4/2011	17	14.0–109.5	12–100	0.01–1.4	0.38–77.0
Vrontamas	10/2007–4/2011	21	8.5–131.2	12–429	0.07–141.6	7.2–221.8

Table 3 Fitted equations of sub-basin flood characteristics.

Catchment	Peak discharge (Q_p) in $m^3 h^{-1}$ (Sharma and Murthy equation)	R^2	Number of flood events
Vivari	$Q_p = 2.265 \left(\frac{T_v}{D}\right)^{1.0687}$	0.808	14
Oinountas Vasaras	$Q_p = 4.13 \left(\frac{T_v}{D}\right)^{0.969}$	0.813	8
Oinountas Kladas	$Q_p = 3.6 \left(\frac{T_v}{D}\right)^{0.954}$	0.827	19
Rasina Koumousta	$Q_p = 0.92 \left(\frac{T_v}{D}\right)^{1.062}$	0.897	19
Rasina airport	$Q_p = 1.092 \left(\frac{T_v}{D}\right)^{0.88}$	0.961	17
Vrontamas	$Q_p = 2.059 \left(\frac{T_v}{D}\right)^{1.1586}$	0.841	21

is the simulated flow in mm. S is estimated as the maximum difference of precipitation minus flow depth ($\max(P-F)$) of the flood events (Table 2) and is related to the flood CN number through the equation

$$CN = \frac{25,400}{S + 254} \tag{3}$$

Figure 4 shows rainfall in relation to flow simulated by Eq. 2 in the Oinountas and Rasina sub-catchments, with curves representing lines of equal CN values superposed. It is clear that the data points do not follow a single CN curve in either basin. This is interpreted as due to the high variability in the rainfall pattern and in antecedent moisture conditions, and suggests the CN number approach may have limited applicability when applied at the whole-catchment scale in the Evrotas with the existing data availability.

2 Application of the SWAT model

2.1 Model estimation

Extending our investigation of the flood response of the Evrotas basin, we apply the semi-distributed SWAT model to generate flood estimates. SWAT has been used successfully in modelling the hydrology of many large catchments (Schuol and Abbaspour 2006, Kannan *et al.* 2007, Mulungu and Munishi 2007, Baffaut and Benson 2009, Betrie *et al.* 2011, Oeurng *et al.* 2011, Nikolaidis *et al.* 2012). The model accounts for the effect of flooding on precipitation, antecedent moisture conditions and the variability of slopes, land uses and soils. In the model, a component representing daily soil moisture accounting is an important moderator of the simulated flood response. The soil moisture accounting is distributed over hydrologic response units (HRUs), each defined as a small sub-basin. The SWAT soil moisture routine takes into consideration several processes such as plant uptake of water, macropore and micropore drainage, evaporation, redistribution between soil layers, lateral drainage, and groundwater infiltration. The spatially distributed daily precipitation which drives the model is estimated within the SWAT model by interpolating from point measurements and taking account of orographic effects (Neitsch *et al.* 2005). SWAT includes parameters with clear physical meaning which are determined from direct field measurements such as soil porosity and aquifer hydraulic conductivity. Also SWAT gives a clear picture of basin drainage features, taking into account the nonlinearity of hydrological processes and drainage basin features. As a distributed model, SWAT requires catchment characteristics in order to generate a flood response. The STRM 90 data (Reuter *et al.* 2007) were used to develop the necessary Digital Elevation Model (DEM). The land use types of the study area were extracted from Corine Land Cover 2000 (CLC 2000). Geographic Information System (GIS) thematic maps of the

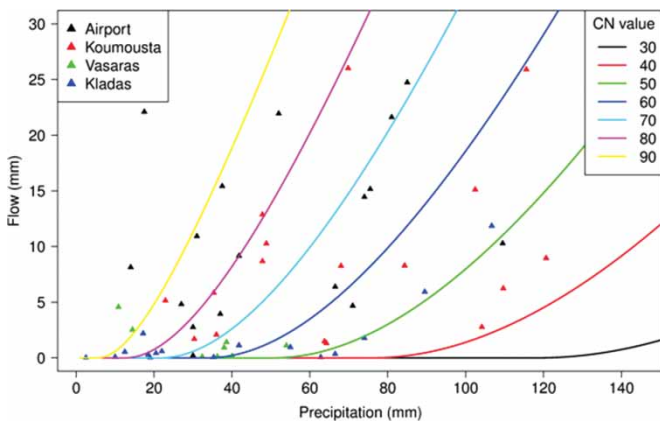


Figure 4 CNs for the Rasina and Oinountas sub-basins.

hydrological network, geology, soils, and slopes were created or provided by the Regional Unit of Lakonia.

In order to apply the SWAT model, the basin was delineated into 150 sub-basins which were further subdivided into homogeneous HRUs. The smallest area of the sub-basin selected was 5 km². Three slope classes were selected 0–5° (9.63% of watershed area), 5–15° (24.49% of watershed area) and >15° (65.88% of watershed area). The irrigation rate used was estimated from the electricity consumption for agricultural water pumping and by the Blaney–Criddle method of evapotranspiration (Tzoraki et al. 2011).

Water levels measured at a 15 min interval from the six stage measurement stations were averaged to a one-day interval and were used to estimate the daily flow in m³ s⁻¹ using a rating curve equation for each station. The absence of a permanent weir structure in the various gauging stations led to errors in the flow estimation of the rating curve. In order to quantify these errors, the Root Mean Square Error of flow of the rating curve for each station was estimated as follows: Vivari station was 0.85 m³ s⁻¹, Vrontamas 1.07 m³ s⁻¹, Rasina Airport 0.228 m³ s⁻¹, Rasina Koumousta 0.168 m³ s⁻¹, Oinountas Vasaras 0.04 m³ s⁻¹ and Oinountas Kladis 0.125 m³ s⁻¹. Daily precipitation data were interpolated using measurements from the stations of Riviotissa (887 mm, mean annual precipitation), Vrontamas (557 mm), Perivolia (1311 mm), Sellasia (849 mm) and Vasaras (758 mm) (Figure 1). The SWAT model was calibrated for the period 2007–2010 using daily flow measurements. The comparison between observed and simulated runoff yielded Nash–Sutcliffe efficiency (NSE) values of 0.69 for Vrontamas, 0.49 for Vivari, 0.56 for Oinountas Vasaras, 0.18 for Rasina Koumousta and 0.57 for Rasina Airport. The model was validated for the period 2004–2007 using monthly flow data. This yielded NSE values of 0.57 for Vrontamas and 0.66 for Vivari. These values were within the acceptable levels reported in the literature (Moriassi et al. 2007). Figure 5 shows the calibrated and validated simulated flow of Vivari and Vrontamas stations. The calibration and validation process of the SWAT model in the Evrotas basin is described in detail by Gamvroudis et al. (2012).

The SWAT model uses the CN approach to generate runoff estimates within hydrological units, and these simulations are then aggregated to give distributed estimates of flow throughout the flow network. This contrasts with the lumped approach used in the previous section. The CN defined within each HRU of SWAT is based on land use, soil type and soil moisture conditions. For instance the suggested default average CN value (SCS runoff CN for moisture condition II) for forest ranges from 40 up to 55, for apple orchards the CN was set to 50, for olives and grassland and wheat in the interval 40–55. The CNs used in SWAT for the Evrotas basin were much lower than CNs used to simulate the lower Nestos river basin (actual CN2 values used 71–82) by Boskidis et al. (2012) and to model the Wenyu (CN2 43–96) (Zhang et al. 2011).

After calibration against field data, we used the SWAT model in the Evrotas first to generate interpolated daily precipitation

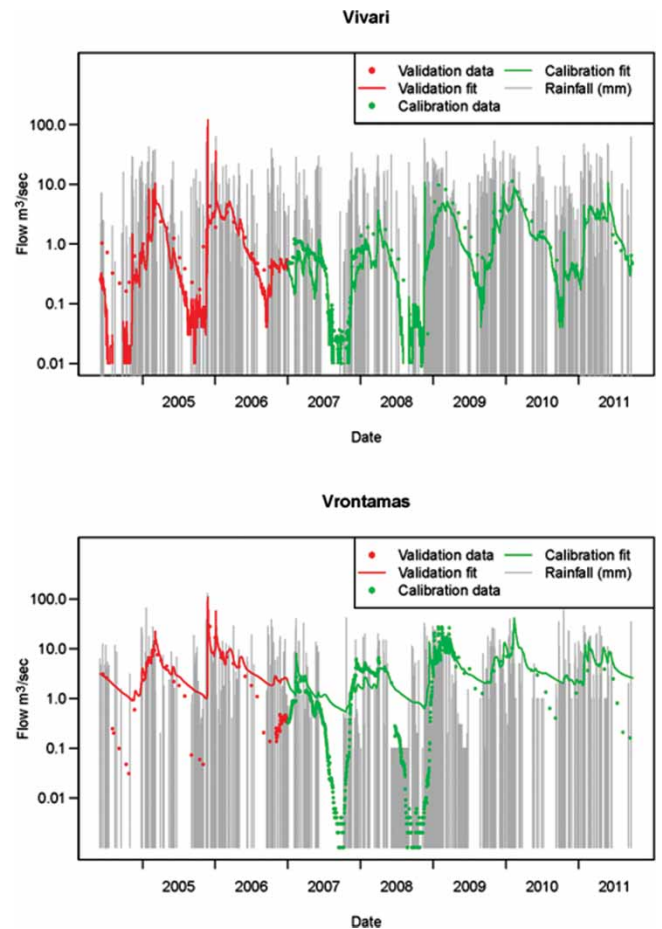


Figure 5 SWAT simulated and observed flow for Vrontamas and Vivari main gauging stations.

and antecedent soil moisture time-series and second to fill gaps in historic flood data since the available high frequency data date only from 2007.

2.2 Simulation of historic flows

After calibration, the SWAT model was used to estimate the hydrographs of the six gauging sites for the period October 1970–August 2011. The historical monthly flow records of Vrontamas were used for comparison with SWAT model simulations in the earlier decades. Also the high peak flows of known hazardous floods of 2003 and 2005 were used for the verification of high floods reconstruction by the SWAT model. Kirkby et al. (2011) suggested that differences in monthly flow duration curves can be used to classify the characteristic signatures of climate and the contrasting hydrological regimes that are driven by climatic differences. The flow-probability relationship of monthly flows for the complete simulation period at the six stage monitoring sites is presented as a log-normal plot in Figure 6, differentiating the hydrological characteristics of each river reach. The stations maintain the same characteristic flow distribution order (less steep in the main stream in comparison to tributaries).

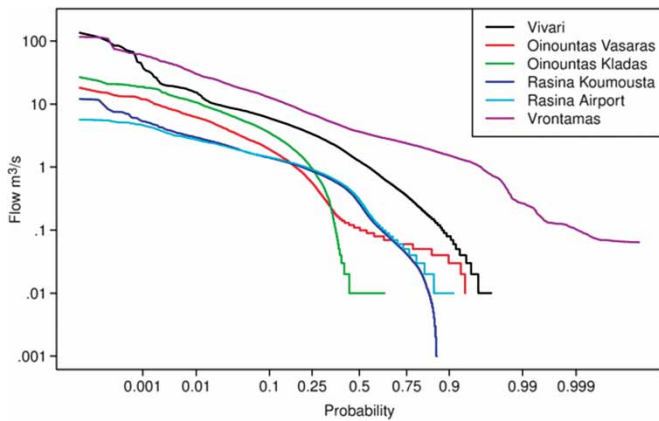


Figure 6 Lognormal plots of simulated flows by the SWAT model (period 1970–2011).

3 Flood classification and seasonality

3.1 Classification

We used the distribution of floods simulated by SWAT for 1970–2011 to characterize the flood distribution at the six gauging sites. Since the data used are simulations of floods rather than measured data, there is an inherent associated uncertainty due to parameter estimation, initial conditions and model structure. We have not fully characterized this uncertainty in our analysis, but believe our approach provides a methodology and baseline for estimating flood characteristics in catchments such as the Evrotas where data are limiting and flow pathways are complex. The goodness-of-fit of model calibration and the associated errors in the simulation suggest that the model was able to capture the hydrologic response of the watershed. In order to classify floods, Ouarda *et al.* (2006) and Sarhadi and Modarres (2011) applied the Peak-Over-Threshold (POT) approach in both wet and arid areas to determine seasonality, identifying the role of hydrologically homogenous regions. Given a continuous time series of flow, the POT events can be defined as (Ouarda *et al.* 2006)

$$\begin{aligned} \xi_t &= 0; & Q_t &\leq Q_B, \\ \xi_t &= Q_t - Q_B; & Q_t &\geq Q_B. \end{aligned} \quad (4)$$

In Eq. 4, Q_B is the base level (or threshold), and ξ_t is the exceedance at time t . The inflection points of the flow duration curves identify the extreme flows and may be selected as base thresholds

(Q_B). The base threshold was evaluated by field studies (Gamvroudis *et al.* 2012), who identified that high flows with probability lower than 0.1 initiate erosion processes, increasing suspended sediment concentration into the water and mobilizing significant sediment loads into the basin.

Based on the concept of the POT method, we suggest the flood duration as the second threshold, and recommend the use of the ‘PDOT’ method (Peak-Duration Over Threshold). In the PDOT model, three flood types are classified that exceed the base level (satisfy Eq. 4) and combine flow and duration thresholds: ‘usual’, ‘ecological’ and ‘hazardous’ (Table 4). The ‘usual’ floods are small-scale events generated by low intensity precipitation and appear to have limited erosion potential. The ‘ecological’ floods may overtop bank height transporting nutrients and playing a vital role in riparian ecology. The ‘hazardous’ floods with their high volumes and duration release sufficient stream power threatening human life and property.

The PDOT method consists of plotting the cumulative mean number of floods exceeding thresholds, $F(t)$, in a time interval $(0, t)$ here equal to a single hydrologic year, against the time t , for each station, and as duration and peak-flow thresholds combination. Any change in slope of $F(t)$ plots indicates variation of flood events and allows sites to be grouped into regions that are homogenous in seasonal flood distribution. Since each flood event within each flood type is different, average hydrographs have been determined for each flood type to show the general shape of the hydrographs per year.

The implementation of the PDOT method in the Evrotas river demands the proper selection of duration and ecological thresholds. The duration (D_e) threshold for the Evrotas basin is extracted by the analysis of historical hazardous floods. A flood atlas of previous hazardous floods in the basin has been created in a study by Nikolaidis (2009). There are records of the location of areas affected by floods in the past in the Evrotas basin, and we use these to select the duration threshold for the basin. The ecological threshold (Q_e) was estimated using Parker’s (2004) equation:

$$Q_e = 3.732 B_{bf} H_{bf} \sqrt{g H_{bf} S} \left(\frac{H_{bf}}{D_{s50}} \right)^{0.2645}, \quad (5)$$

where B_{bf} is the bankfull width (m), H_{bf} the bankfull depth (m), S is stream slope (–), g the acceleration of gravity (9.81 m s^{-2}) and D_{s50} (m) the bed surface median grain size.

Table 4 The four flood types according to PDOT method.

Duration threshold (days)	Flow threshold ($\text{m}^3 \text{ s}^{-1}$)	Duration	Magnitude	Flood class
$D < D_e$	$Q_t < Q_b$	Short	Small to medium	Usual
$D < D_e$	$Q_b \leq Q_t < Q_e$	Short	Medium to large	Ecological
$D \geq D_e$	$Q_b \leq Q_t < Q_e$	Long	Medium to large	Ecological
$D \geq D_e$	$Q_t \geq Q_e$	Long	Large	Hazardous

In the Koiliaris river in Crete, the rainfall duration of the range 10–60 h generated six reported extreme overbank flash floods in the period 1988–2009 (Kourgialas *et al.* 2011). Studies at the European level showed that hazardous floods from the Mediterranean and Alpine-Mediterranean area are caused by a rainfall duration between 7 and 34 h (Marchi *et al.* 2010). Therefore, the lag time (the duration between the time of the centroid of the generating rainfall sequence and the time of the discharge peak) of selected flash floods in Europe is estimated to be less than 5 h (Marchi *et al.* 2010). Georgakakos (1986) identified a 6 h lag time as a threshold for flood generation for catchments of 400 km² in the USA. In the UK, a flood event is considered as flashy if it has a time to peak of up to 3 h within a catchment of 5–10 km² (Collier 2007). Even though the short lag time of most studied hazardous floods, the hydrograph duration is higher than two days, since the falling limb of the hydrograph appears to have a long duration. The hydrograph duration of most significant flood events in Assino and Genna sub-catchments in the Upper Tiber River catchment, in Italy was greater than two days (Brocca *et al.* 2011). Flood duration greater than two days was also measured in the Koiliaris river basin in Greece (Kourgialas *et al.* 2011). Since the duration of many historical hazardous floods in the Evrotas is greater than two days, a two days threshold was selected as the threshold hydrograph duration (D_e) for hazardous floods.

This method has been applied to estimate the distribution of usual, ecological and hazardous floods on the Evrotas, using floods simulated by the SWAT model, in the absence of a long record of measured flow data.

The ecological threshold (Q_e) represents significant sediment transport, an inundated floodplain areas and high hazardous risk, and is estimated as the flow that corresponds to the banks full discharge and Q_e was estimated using the methodology developed by Parker (2004). Morphological characteristics or Evrotas streams were extracted by DEM in GIS. The value of D_{s50} was calibrated. Initially, the monthly field flow measurements were related to the mean stream depth and a rating curve equation for each studied site was extracted. A full bank depth was extracted by the DEM, and

with the help of the rating curve equation the full bank flow was estimated by

$$Q_{RC,FB} = aH_{FB}^b, \quad (6)$$

where $Q_{RC,FB}$ is the rating curve full bank flow and H_{FB} is the full bank stream water depth. Then, Eq. 5 was used for the estimation of the ecological flow threshold in the same sites, selecting a D_{s50} (mm) value that minimized the absolute difference between the rating curve full bank flow and the ecological threshold ($|Q_{RC,FB} - Q_e|$). The Excel add-in Solver was used for the selection of D_{s50} value. For Vivari and Rasina, the resulting values were 0.016 and 0.011 m and these values were used for all corresponding upstream sub-catchments of the Taygetos mountains. At Kladas, the value was 0.021 m that was used for the whole Parnonas range, and finally for the main stream the value of 0.105 m was estimated from analysis of data from the Vrontamas site. The ecological threshold (Q_e) was validated for the Rasina stream using the HEC-GeoRAS (US Army Corps of Engineers 2009) program by applying a digital terrain model extracted by detailed topographic studies in the site. The Parker equation is strongly dependent on the D_{s50} value since the remaining parameters are based on geography. Monte Carlo analysis was carried out for this parameter. The range of the parameter and the resulted ecological flow are shown in Table 5. For instance, in Vivari, the ecological flow was estimated by surfer analysis as 71 m³ s⁻¹, with a D_{s50} of 0.016 m, the following Monte Carlo analysis has given a value of ecological flow 75.2 m³ s⁻¹ ranging between 70.7 and 79.8. For the estimation of flood classes, we selected the minimum ecological flow derived by Monte Carlo analysis.

Figure 7 (left) shows the spatial distribution of the ecological flows in the basin (5.0–186.5 m³ s⁻¹). Some tributaries of the Taygetos show very low-bankfull flows, due largely to their steep slopes and narrow river bed morphology. Figure 7 (right) shows the catchment status during the high peak flow of the major flood of 25 November 2005, as simulated by the SWAT model. It is clear that the simulated flood developed from the north-west part of the basin and higher flows are simulated in

Table 5 Ecological flow estimation.

Site	Rating curve, $Q_{RC,FB} = aH_{FB}^b$		Q_e -surfer	D_{s50} (m)	Q_e -Monte Carlo	Q_e , min-Monte Carlo	Q_e , max-Monte Carlo
	a	b					
Vivari	30.16	2.28	71	0.016	75.2	70.7	79.8
Oinounas Vasaras	12.385	2.187	97.2	0.021	97.8	97.2	98.4
Oinounas Kladas	27.7	2.585	60.8	0.021	61.2	60.8	61.6
Rasina Koumousta	64.657	3.483	5.4	0.011	5.4	5.4	5.4
Rasina airport	117.5	3.46	26.5	0.011	26.1	25.8	26.4
Vrontamas	25.14	2.265	169.9	0.105	171.4	169.4	173.6

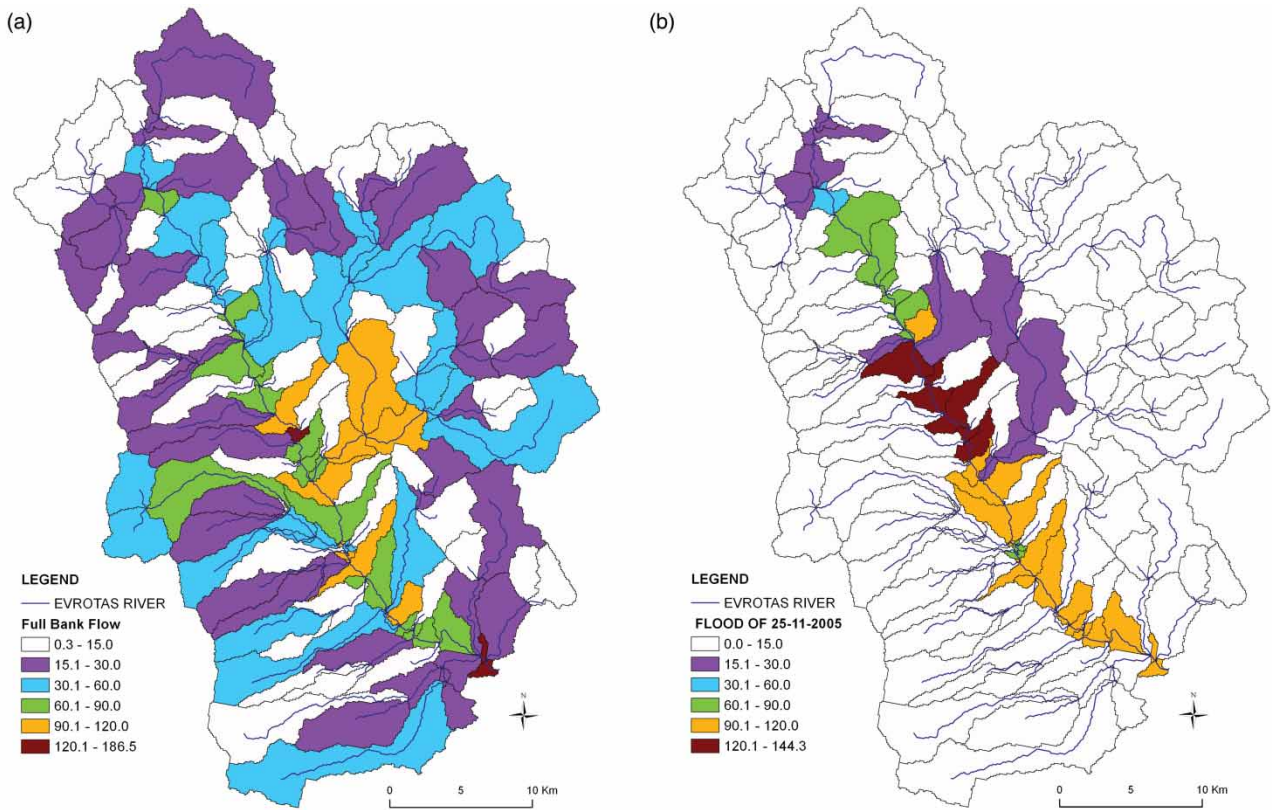


Figure 7 (a) The ecological flow or bankful discharge of the Evrotas basin (left) and the peak flow of the serious flood event of 25 November 2005 simulated by SWAT (right). (b) The ecological flow or bankful discharge of the Evrotas basin (left) and the peak flow of the serious flood event of 25 November 2005 simulated by SWAT (right).

the main stream. There is high simulated flow variability ($0.0-144.3 \text{ m}^3 \text{ s}^{-1}$) and the peak flows exceed the ecological flow in some parts of the main stream, especially the upstream area of Sparta.

At Oinountas Koumousta and Oinountas Kladas, there were no hazardous floods during the 40 years of simulated flow analysis. Simulations suggest the Rasina stream has experienced hazardous floods in its upper part (in Rasina Koumousta) in the 1970s and 1980s. However, the areas vulnerable to flooding are the main stream of the Evrotas basin from Vivari as far as Vrontamas, and the area upstream of Sparta has the highest flood risk. Therefore, flood analysis was focused in the main stream, where a significant number of historical events have

been recorded. The flood events were separated and by using the flow and duration thresholds, the different flood types were identified and the frequency of each flood class estimated at each site. Ecological floods are, in general, dominant in all streams and tributaries of the Evrotas basin (Table 6), that is to say, the flood events last less than two days and the river flow is usually less than the ecological flow. In the main stream in the vicinity of Vivari, where many villages and agricultural fields are located, 5% of floods are classified as hazardous. This figure increases downstream and in the Vrontamas area just before the start of the karstic gorge increases to 7%. Figure 8 (right part) shows the spatial distribution of ecological and hazardous flood classes for the events of 27 January 2003

Table 6 Flood thresholds at each site.

	Base level flow (Q_b) (cm)	Duration (D_e) (days)	Ecological flow (Q_e) (cm)	Flood class frequency		
				Usual	Ecological	Hazardous
Vivari	6.0	2	70.7	0.51	0.44	0.05
Main stream	8.9	2	81.0	0.37	0.56	0.07
Vrontamas	12.7	2	169.4	0.29	0.68	0.07
Rasina Koumousta	1.4	2	5.4	0.05	0.90	0.05

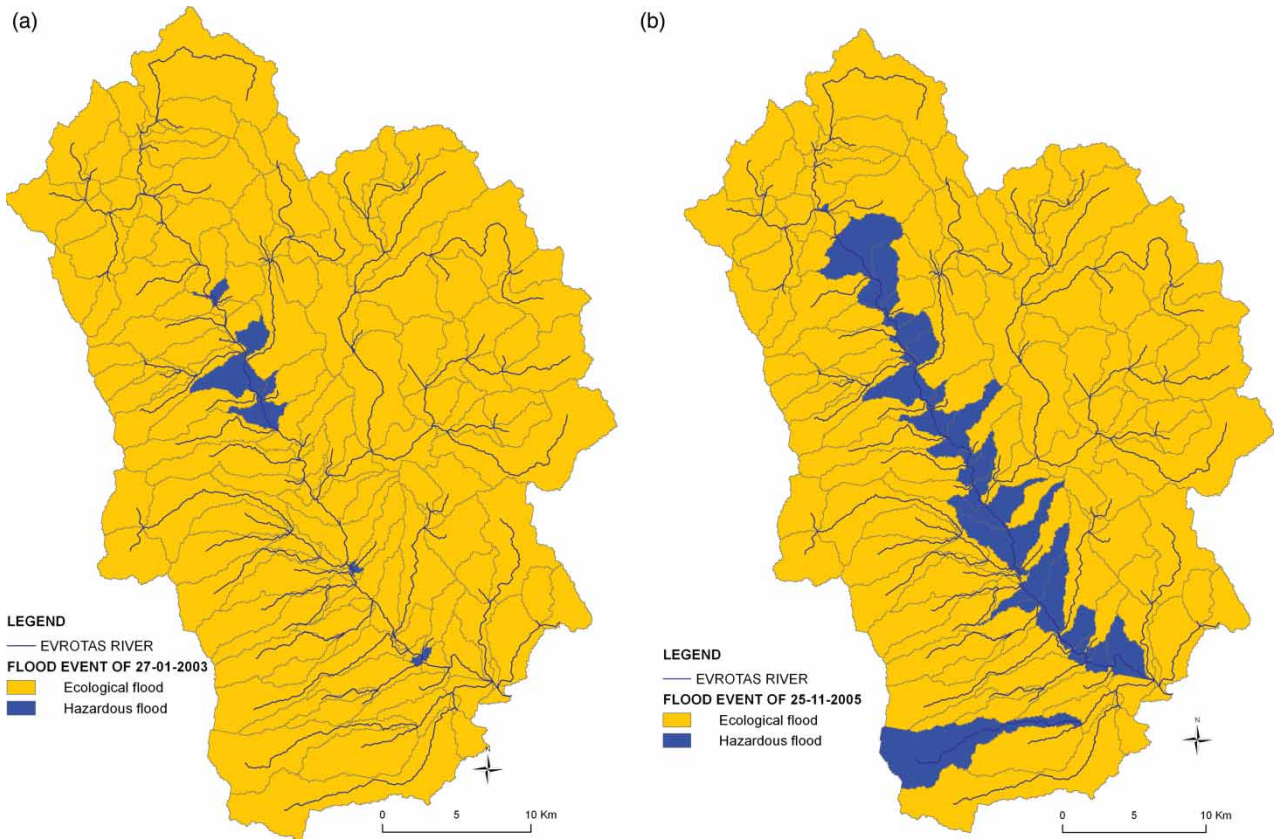


Figure 8 (a) Flood type characterization of simulated flood events of 27 January 2003 (right part) and 25 November 2005 (left part). (b) Flood type characterization of simulated flood events of 27 January 2003 (right part) and 25 November 2005 (left part).

and 25 November 2005. On 27 January 2003, hazardous flooding was mainly in the area close to Vivari, but in contrast during the event of 25 November 2005, flooding not only extended to the main stream but also included some tributaries. Figure 8 (left part) shows the high flood risk of the Evrotas main stream (between Sparta and Vrontamas) and a potential delineation of the basin into areas liable to floods. Overland flow from the whole basin and the tributaries is collected in the main stream which drains the alluvial basin and is more vulnerable to flooding.

3.2 Seasonality

Flood seasonality of daily simulated flow data were estimated using the PDOT duration method. Stations with similar seasonal partitioning of the year are grouped into seasonality homogenous regions. As shown in Figure 9(a), not only the main stream of Evrotas, but also its tributaries could be considered as a hydrologically homogenous region and that two seasons can adequately describe the seasonality. The first is from October to March and the second from March to September. A similar flood seasonality

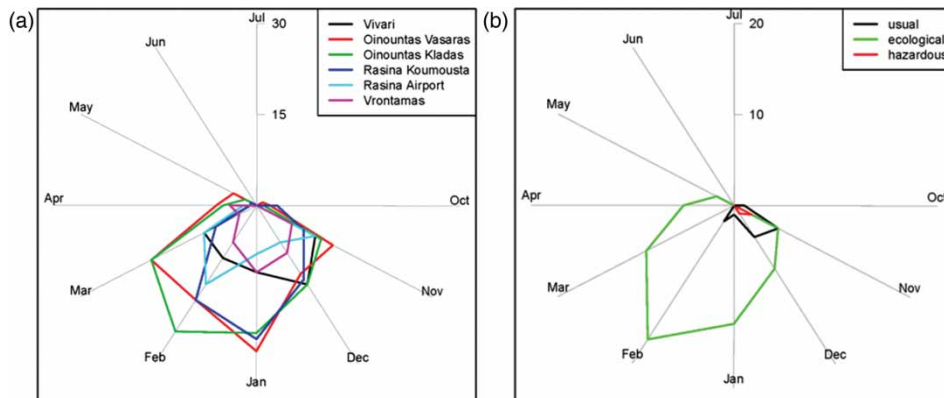


Figure 9 (a) Flood seasonality in the Evrotas (units 15 and 30). (b) Flood seasonality according to the PDOT method at Vrontamas station for different flood classes.

pattern occurred in 14 basins in Halilrud catchment in Southeastern Iran studied by Sarhadi and Modarres (2011), but the first season is initiated two months later than in the Evrotas. Studying the flood classes of each station, we see that these seasons are different and each flood class has distinct seasons. For instance, at Vrontamas, the ‘usual’ flood occurs up to February, and ecological floods up to May (Figure 9(b)).

We have averaged the flow per month to create a Flood Status Frequency Graph (FSFG). This time scale gives an average image of the monthly fluctuations in river discharge (Gallart *et al.* 2011). The FSFGs of the selected sites (Figure 10) show the percentages of each flood class per month. For instance, the Vivari FSFG shows that, from July until September the base floods (i.e. no flooding) are dominant, while from October until March hazardous floods are more common, up to

100% of the time in January. In the main stream, the hazardous floods are around 50% of the time in November. Ecological Flood Class is significant in Vivari and in the main stream but not in Vrontamas. Also the study of Diakakis *et al.* (2012) showed seasonality patterns of 545 hazardous flood events over the last 130 years in Greece with more events clustering in November.

The FSFG graph of the Evrotas hazardous floods (Vrontamas site) may be compared with the Europe-wide graph in the work of Marchi *et al.* (2010) of the HYDRATE project. Hazardous floods in Evrotas occur more frequently in the period of November to March due to distribution of precipitation around the year (southern Mediterranean depressions) in contrast to the Europe-wide floods that occur from July to October (Gaume *et al.* 2009).

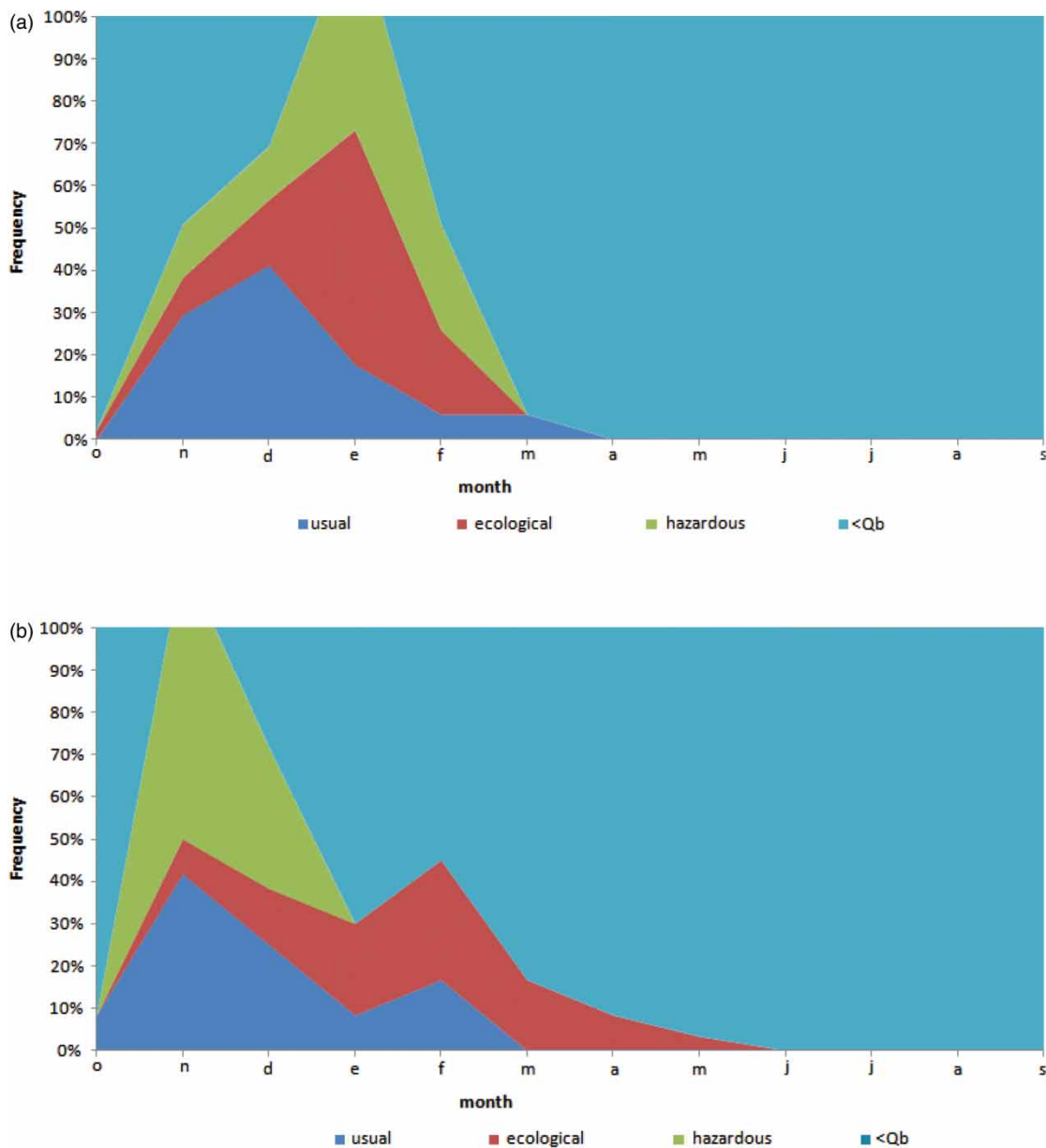


Figure 10 (a) Flood status frequency graph at (a) Vivari and (b) Vrontamas.

The different flood types can be related to the main flood variables such as hydrograph duration and flood volume. The equations in Table 4 can be used to estimate the peak flow in relation to flood volume and hydrograph duration. For instance, if a flood volume of 2 hm³ (equivalent to 5.1 mm in runoff for Vivari and 1.5 mm for Vrontamas) is generated by a storm which results in less than 15 h hydrograph duration in Vivari and less than 25 h in Vrontamas, then the flow overtops the river banks and starts to flood. In general, hazardous floods are of short duration. A flood volume of 2 hm³ needs to last over 20 h in order not to create a hazardous flood.

4 Conclusions

Like many Mediterranean rivers, the Evrotas and its tributaries are karstic and temporary. Rainfall is highly spatially variable, and sparsely recorded. Flow data are limited, particularly during floods. With so many sources of uncertainty, the rainfall–runoff response is difficult to characterize. We have used hourly stage measurements over 2007–2011 at six sites to identify some of the main features of the hydrological response in the Evrotas. We have shown that a simple CN approach applied to storm events at the sub-catchment scale gives very poor estimates of flow. High karst infiltration rates, variable antecedent moisture conditions, spatially variable rainfall and catchment characteristics such as geology, slopes and land-use play a dominant role in generating the shape of the hydrograph. There is no observed linearity between flow and precipitation and the generated runoff volumes are strongly variable in time and the measured precipitation amount.

We have extended the flow record at the Evrotas using the SWAT model to cover the period 1970–2011 using the available rainfall record over this period. While recognizing the uncertainty inherent in this extrapolation, we have set forward a methodology for estimating the distribution of ‘usual’, ‘ecological’ and ‘hazardous’ floods in the Evrotas basin, and their seasonal distribution. Presentation of flood types in radar and FSFGs plots gives a good visualization of flood seasonality. In the Evrotas, the seasonality pattern of hazardous floods is in agreement with other studies in Greece and differs from other major European floods. The frequency of hazardous floods in the main stream is estimated from 5% to 7% of the total floods and much lower in some tributaries. Ecological floods with duration more than two days are the dominant flood type of the basin.

Acknowledgements

The study was carried out within the MIRAGE project, EC Priority Area ‘Environment (including Climate Change)’, contract number 211732. The authors are grateful to the Department of Environment and Hydrology, Region of Peloponnesus, Regional

Unit of Lakonia for providing monthly flow data from 1970 to 2011, and daily rainfall data for this period.

References

- Antonakos, A. and Lambrakis, N., 2000. Hydrodynamic characteristics and nitrate propagation in Sparta aquifer. *Water Research*, 34 (16), 3977–3986.
- Arnold, J.G., et al., 1988. Large area hydrologic modeling and assessment: Part I. Model development. *The Journal of the American Water Resources Association*, 34 (1), 73–89.
- Baffaut, C. and Benson, V.W., 2009. Modeling flow and pollutant transport in a karst watershed with SWAT. *American Society of Agricultural and Biological Engineers*, 52 (2), 469–479.
- Belmonte, A.M.C. and Beltrán, F.S., 2001. Flood events in Mediterranean ephemeral streams (ramblas) in Valencia region. *Spain*, 10 (3), 282–290.
- Betrie, G.D., et al., 2011. Sediment management modelling in the blue Nile basin using SWAT model. *Hydrology and Earth Sciences*, 15, 807–818.
- Bicknell, B.R., et al., 2001. Hydrological simulation program – FORTRAN (HSPF): user’s manual – version 12. Athens, Georgia: National Exposure Research Laboratory. Office of Research and Development. U.S. Environmental Protection Agency.
- Boskidis, I., et al., 2012. Hydrologic and water quality modeling of lower Nestor river basin. *Water Resource Management*, 26 (10), 3023–3051.
- Brocca, L., Melone, F., and Moramarco, T., 2011. Distributed rainfall-runoff modelling for flood frequency estimation and flood forecasting. *Hydrological Processes*, 25, 2801–2813.
- Collier, C.G., 2007. Flash flood forecasting: what are the limits of predictability? *Quarterly Journal of the Royal Meteorology Society*, 133, 3–23.
- Diakakis, M., Mavroulis, S., and Deligiannakis, G., 2012. Floods in Greece, a statistical and spatial approach. *Natural Hazards*, 62 (2), 485–500.
- Fohrer, N., et al., 1999. Changing soil and surface conditions during rainfall single rainstorm/subsequent rainstorms. *Catena*, 37 (3), 355–375.
- Gallart, F., et al., 2008. Investigating hydrological regimes and processes in a set of catchments with temporary waters in Mediterranean Europe hydrological sciences. *Journal des Sciences Hydrologiques*, 53, 618–628.
- Gamvroudis, C., et al., 2013. Sediment transport modeling of a large temporary river basin. *Journal of hydrology*, In review.
- Gaume, E., et al., 2009. A compilation of data on European flash floods. *Journal of Hydrology*, 367, 70–78. 10.1016/j.jhydrol.2008.12.028.
- Georgakakos, K.P., 1986. On the design of national, real-time warning systems with capability for site-specific, flash flood

- forecasts. *Bulletin of the American Meteorological Society*, 67 (10), 1233–1239.
- Hawkins, R., *et al.*, 2009. *Curve number hydrology: state of the practice/prepared by the ASCE/EWRI curve number hydrology task committee sponsored by Environmental and Water Resources Institute (EWRI) of the American Society of Civil Engineers*, Virginia. 106. ISBN 978-0-7844-1004-2.
- Kannan, N., *et al.*, 2007. Hydrological modelling of a small catchment using SWAT-2000 – Ensuring correct flow partitioning for contaminant modelling. *Journal of Hydrology*, 334, 64–72.
- Kirkby, M.J., *et al.*, 2011. Classifying low flow hydrological regimes at a regional scale. *Hydrology and Earth System Sciences*, 15, 3741–3750.
- Kourgialas, N., Karatzas, G., and Nikolaidis, N.P., 2010. An integrated framework for the hydrologic simulation of complex geomorphological river basin. *Journal of Hydrology*, 381, 308–321.
- Kourgialas, N., Karatzas, G., and Nikolaidis, N.P., 2011. Development of a thresholds approach for real-time flash flood prediction in complex geomorphological river basins. *Hydrological Processes*, 26 (10) 1478–1494.
- Marchi, L., *et al.*, 2010. Characterisation of selected extreme flash floods in Europe and implication for flood risk management. *Journal of Hydrology*, 39, 118–133.
- McIntyre, N., Al-Qurashi, A., and Wheeler, H., 2007. Regression analysis of rainfall-runoff data from an arid catchment in Oman. *Hydrological Sciences. Special section: Dryland Hydrology in Mediterranean Regions*, 52 (6), 1103–1118.
- Moraetis, D., *et al.*, 2011. High-frequency monitoring for the identification of hydrological and bio-geochemical processes in a Mediterranean river basin. *Journal of Hydrology*, 389 (1–2), 127–136.
- Moriassi, D.N., *et al.*, 2007. Model evaluation guidelines for systematic quantification of accuracy in watershed simulations. *Transactions of the ASABE*, 50, 885–900.
- Mulungu, D. and Munishi, S., 2007. Simiyu river catchment parameterization using SWAT model. *Physics and Chemistry of the Earth*, 32, 1032–1039.
- Neitsch, S.L., *et al.*, 2005. *Soil and water assessment tool: theoretical Documentation-Version 2005*. Temple, TX: Grassland, Soil and Water Research Laboratory. Agricultural Research Service.
- Nikolaidis, N.P., *et al.*, 2009. Management plans of Evrotas River Basin. In: N.P. Nikolaidis, N. Kalogerakis, N. Skoulikidis, K. Tsakiris, (eds). 2005–2009. *Environmental friendly technologies for rural development, program life-environment, LIFE05ENV/Gr/000245 EE (EnviFriendly)*, Technical Notes, 122.
- Nikolaidis, N.P., Hu, H., and Ecsedy, C., 1994. Effects of climatic variability on freshwater watersheds. case studies. *Aquatic Sciences*, 56 (2), 161–178.
- Nikolaidis, N.P., Bouraoui, F., and Bidoglio, G., 2012. Hydrologic and geochemical modelling of a karstic Mediterranean watershed. *Hydrology and Earth System Sciences Discussions*, 9, 1–27.
- Nikolopoulos, E.I., *et al.*, 2011. Sensitivity of a mountain basin flash flood to initial wetness condition and rainfall variability. *Journal of Hydrology*, 402 (3–4), 165–178.
- Oeurng, C., Sauvage, S., and Sánchez-Pérez, J.M., 2011. Assessment of hydrology and particulate organic carbon yield in a large agricultural catchment using the SWAT model. *Journal of Hydrology*, 401, 145–153.
- Ouarda, T.B.M.J., *et al.*, 2006. Data-based comparison of seasonality-based regional flood frequency methods. *Journal of Hydrology*, 330, 329–339.
- Parker, G., 2004. *A tool from the NCED stream restoration toolbox: the gravel river bankfull discharge estimator*. National Center for Earth – Surface Dynamics, Stream Restoration Program, Enabling Landscape Sustainability.
- Reuter, H.I., Nelson, A., and Jarvis, A., 2007. An evaluation of void filling interpolation methods for SRTM data. *International Journal of Geographic Information Science*, 21 (9), 983–1008.
- Rimmer, A. and Salinger, Y., 2006. Modelling precipitation-streamflow processes in karst basin: the case of the Jordan river sources. *Israel. Journal of Hydrology*, 331, 524–542.
- Sarhadi, A. and Modarres, R., 2011. Flood seasonality – based regionalization methods: a data-based comparison. *Hydrological Processes*, 25, 3613–3624.
- Schuol, J. and Abbaspour, K.C., 2006. Calibration and uncertainty issues of a hydrological model (SWAT) applied to West Africa. *Advances in Geosciences*, 9, 137–143.
- Sharma, K.D. and Murthy, J.S.R., 1998. A practical approach to rainfall-runoff modeling in arid zone drainage basins. *Hydrological Sciences Journal*, 43, 331–348.
- Tockner, K., Malard, F., and Ward, J.V., 2000. An extension of the flood pulse concept. *Hydrological Processes*, 14, 2861–2883.
- Tzoraki, O., *et al.*, 2007. Modeling of in-stream biogeochemical processes of temporary rivers. *Hydrological Processes*, 23 (2), 272–283.
- Tzoraki, O., *et al.*, 2011. Hydrological modeling of an intense carstified river system. N. Lambrakis *et al.* (Eds.), *Advances in the Research of Aquatic Environment*, Vol. 1, DOI 10.1007/978-3-642-19902-8, Springer-Verlag Berlin Heidelberg 2011.
- US Army Corps of Engineers, 2009. *HEC – GeoRAS, GIS tools for support of HEC-RAS using Arc-GIS, user manual*. Institute for Water Resources, Hydrologic Engineering Center. http://www.hec.usace.army.mil/software/hec-ras/documents/HEC-GeoRAS42_UsersManual.pdf
- Van Lanen, H.A.J., Tallaksen, L.M., and Rees, G., 2007. Annex II. Droughts and climate change. In: *Commission Staff Working Document Impact Assessment (SEC(2007) 993)*.

- Accompanying document to communication addressing the challenge of water scarcity and droughts in the European Union (COM(2007) 414). Brussels, Belgium: Commission of the European Communities.
- Vivoni, E.R., et al., 2006. Analysis of a monsoon flood event in an ephemeral tributary and its downstream hydrologic effects. *Water Resources Research*, 42 (3), W03404.
- White, E. D. et al., 2011. Development and application of a physically based landscape water balance in the SWAT model. *Hydrological Processes*, 25 (6), 915–925.
- Zhang, Y., et al., 2011. Water quantity and quality optimization modeling of dams operation based on SWAT in Wenyu river catchment, China. *Environmental Monitoring and Assessment*, 173, 409–430. Available from: <http://dx.doi.org/10.1007/s10661-010-1396-5>.